

# Polarization and Experimental Configuration Analysis of Sum Frequency Generation Vibrational Spectra of Air/Water Interface

Wei Gan<sup>†</sup>, Dan Wu<sup>†</sup>, Zhen Zhang<sup>†</sup>, Ran-ran Feng<sup>†</sup>, and Hong-fei Wang<sup>\*</sup>

State Key Laboratory of Molecular Reaction Dynamics,  
Institute of Chemistry, the Chinese Academy of Sciences, Beijing, China, 100080

(Dated: March 14, 2021)

Here we report a detailed study on spectroscopy, structure and dynamics of water molecules at air/water interface, investigated with Sum Frequency Generation Vibrational Spectroscopy (SFG-VS). Quantitative polarization and experimental configuration analysis of the SFG data in different polarizations with four sets of experimental configurations can shed new lights on our present understanding of the air/water interface. Firstly, we concluded that the motion of the interfacial water molecules can only be in a limited angular range, instead rapidly varying over a broad angular range in the vibrational relaxation time suggested previously. Secondly, because different vibrational modes of different molecular species at the interface has different symmetry properties, polarization and symmetry analysis of the SFG-VS spectral features can help assignment of the SFG-VS spectra peaks to different interfacial species. These analysis concluded that the narrow  $3693\text{cm}^{-1}$  and broad  $3550\text{cm}^{-1}$  peaks belong to  $C_{\infty v}$  symmetry, while the broad  $3250\text{cm}^{-1}$  and  $3450\text{cm}^{-1}$  peaks belong to the symmetric stretching modes with  $C_{2v}$  symmetry. Thus, the  $3693\text{cm}^{-1}$  peak is assigned to the free OH, the  $3550\text{cm}^{-1}$  peak is assigned to the single hydrogen bonded OH stretching mode, and the  $3250\text{cm}^{-1}$  and  $3450\text{cm}^{-1}$  peaks are assigned to interfacial water molecules as two hydrogen donors for hydrogen bonding (with  $C_{2v}$  symmetry), respectively. Thirdly, analysis of the SFG-VS spectra concluded that the singly hydrogen bonded water molecules at the air/water interface have their dipole vector direct almost parallel to the interface, and is with a very narrow orientational distribution. The doubly hydrogen bond donor water molecules have their dipole vector point away from the liquid phase.

## I. INTRODUCTION

Interfaces of water are the most important subjects not only because water is widely involved in physical, chemical, environmental as well as biological processes, but also because water is so far the most mysteries molecule in the universe.<sup>1,2,3,4</sup> Among them, air/water interface has been intensively investigated theoretically or experimentally over the last decades. Spectroscopy, molecular structure and dynamics at air/water interface is studied with theoretical analysis such as *ab initio* calculation or molecular dynamics simulation,<sup>5,6,7,8,9,10,11,12,13</sup> or experimental techniques such as X-ray reflection,<sup>14,15</sup> Stimulated Raman Scattering (SRS),<sup>16</sup> Near-edge X-Ray Adsorption Fine Structure (NEXAFS),<sup>17</sup> Second Harmonic Generation (SHG),<sup>18,19</sup> as well as Sum Frequency Generation, etc.<sup>20,21,22,23,24,25,26,27,28</sup> Among these experimental techniques, Second Harmonic Generation and Sum Frequency Generation are the most important methods for molecular interface studies because of their surface sensitivity and specificity.<sup>29,30,31,32,33,34,35,36</sup> With these investigations, the properties of the water molecules at the interface, such as the surface density, surface structure, surface potential as well as surface dynamics, have been intensively discussed.

However, conclusions on the surface molecule species at air/water interface are still under discussion.<sup>17,20,23,25</sup> With SFG-VS experimental studies, the following interfacial water species have been reported in literatures, namely, water molecules straddle at the interface with one OH bond hydrogen bonded to neighboring molecules in liquid phase (singly bonded OH) and another OH bond free from hydrogen bonding (free OH) in gas phase;<sup>22,23,24,37</sup> water molecules with both OH bonds symmetrically hydrogen bonded in a tetrahedral network (ice-like and liquid-like structures);<sup>22,23,24,37</sup> and water molecules in gas phase with both OH bonds not hydrogen bonded pointing into the liquid phase.<sup>23,26</sup> With NEXAFS measurement and *ab initio* molecular dynamics simulation, water molecules with both OH bonds not hydrogen bonded pointing out of the interface was also proposed.<sup>13,17</sup> The latter case is particularly controversial because NEXAFS is not strictly a surface specific technique.<sup>17</sup> With polarization SFG-VS measurement, Wei *et al.* discussed the absence of SFG spectra in some polarization combinations and proposed an explanation through fast orientational motion in a broad range of about  $102^\circ$  in a time scale comparable or less than  $0.5\text{ ps}$ .<sup>25</sup> However, puzzle still remains because some of the experimental studies suggests ordered and slow dynamics for interfaces of hydrogen bonding liquids, while some experimental investigations suggested a more dynamic and less ordered picture for the liquid interfaces, air/water interface included.<sup>33</sup> In addition, whether the surface orientation relaxation is fast or slow than the bulk water molecules is also an issue under discussion in the recent literatures.<sup>12,38,39</sup> Besides

<sup>†</sup>Also Graduate School of the Chinese Academy of Sciences

<sup>\*</sup>Author to whom correspondence should be addressed. E-mail: hongfei@mrdlab.icas.ac.cn. Tel. 86-10-62555347, Fax 86-10-62563167.

SHG and SFG-VS experimental studies,<sup>33,40</sup> Structure and dynamics of water molecules at the air/water interface have also been intensively discussed with theoretical simulations.<sup>5,6,7,8,9,10,11,12,13</sup> Even though with so much efforts and progresses both by experimentalists and theoreticians, our detailed understanding of air/water interface is still limited. Just as indicated by B. C. Garrett recently,<sup>41</sup> ‘...(direct) experiments are difficult to perform because the liquid interface is disordered, dynamic, and small (typically only a few molecules wide) relative to the bulk’.

Actually, direct measurement of the liquid interface is not as difficult as suggested as above. It has been known that along with SHG, SFG-VS can provide direct measurement on liquid interface no other technique can match.<sup>33,40</sup> As pointed out by Miranda and Shen, ‘SFG is currently the only technique that can yield a vibrational spectrum for a neat liquid interface’.<sup>33</sup> In fact, with the advances of ultrafast laser and detection technology in the past decade and especially recent few years,<sup>42,43,44,45</sup> particularly with commercial systems designed for SFG-VS measurement,<sup>46</sup> SFG-VS, as well as SHG, experiments have come from easier to routine.<sup>47</sup> The real difficulty lies on the fact that quantitative analysis and interpretation of the SFG-VS, as well as SHG, data had been not as well developed and widely performed until recently.<sup>25,35,48,49,50,51,52,53,54,55,56,57,58</sup> Therefore, conclusions in many previous reports on the investigations of air/water interface, as well as other liquid interfaces, with SFG-VS are subjected to different interpretations.

As we have demonstrated in a series of recent publications, systematically quantitative treatment to SFG-VS data is not only possible, but also very effective for obtaining detailed spectroscopic, structural and thermodynamic properties of liquid interfaces.<sup>49,50,51,52,53,54,55,56,57,58</sup> In these works, we not only developed methodology for quantitative polarization and experimental configuration analysis in SFG-VS and SHG, we also tested accuracy and sensitivity of some of the methodology. We have applied them to elucidated the anti-parallel double layered structure and thermodynamics of some organic liquid aqueous solution interfaces. In addition, we also demonstrated that a set of polarization selection rules (or guidelines) in SFG-VS can be developed for vibrational spectrum assignment through symmetry analysis of the SFG-VS spectral features.<sup>50,51</sup> This latter approach is extremely useful for discerning complex SFG-VS spectrum with unidentified or controversial assignments. Recently, based on polarization analysis, Ostroverkhov *et al.* demonstrated a phase-sensitive interference analysis of SFG polarization spectra of water/quartz interface.<sup>59</sup> With these development, in this report we intend to apply these analysis methodologies to the study of air/water interface.

In this work, we examined SFG-VS spectra at air/water interface measured in different polarizations under four experimental configurations with polarization

analysis method and experimental configuration analysis. With these analysis, detailed new information are obtained for understanding of the spectroscopy, structure and dynamics of the air/water interface. In the following sections, after a brief introduction of the theoretical background and experimental conditions, we first discuss the motion of the interfacial water molecules at the air/water interface, which was previously suggested experiencing rapidly motion over a broad angular range in the vibrational relaxation time; then we use polarization and symmetry analysis of the SFG-VS spectral features for assignment of the SFG-VS spectra peaks; in the end, we shall discuss the structure and orientation of the water molecules at the air/water interface.

## II. POLARIZATION AND EXPERIMENTAL CONFIGURATION ANALYSIS IN SFG-VS

Quantitative polarization analysis and experimental configuration analysis can provide rich and detailed information of spectroscopy, structure and dynamics of molecular interfaces.<sup>25,35,49,50,51,53</sup> Generally, the SFG intensity in the reflective direction is,<sup>35,50</sup>

$$I(\omega) = \frac{8\pi^3\omega^2 \sec^2\beta}{c^3 n_1(\omega) n_1(\omega_1) n_1(\omega_2)} \left| \chi_{eff}^{(2)} \right|^2 I(\omega_1) I(\omega_2) \quad (1)$$

in which  $\omega$ ,  $\omega_1$  and  $\omega_2$  are the frequencies of the SFG signal, visible and IR laser beam, respectively.  $n_i(\omega_i)$  is the refractive index of bulk medium  $i$  at frequency  $\omega_i$ , and  $n'(\omega_i)$  is the effective refractive index of the interface layer at  $\omega_i$ .  $\beta_i$  is the incident or reflection angle from interface normal of the  $i$ th light beams;  $I(\omega_i)$  is the intensity of the SFG signal or the input laser beam.  $\chi_{eff}^{(2)}$  is the effective second order susceptibility for an interface. The notations and the experiment geometry have been described in detail previously.<sup>35,50</sup>

$\chi_{eff}^{(2)}$  for the four generally used independent polarization combinations can be deduced from the 7 nonzero macroscopic susceptibility tensors for an achiral rotationally isotropic interface ( $C_{\infty v}$ ).<sup>35,50</sup>

$$\begin{aligned} \chi_{eff}^{(2),ssp} &= L_{yy}(\omega) L_{yy}(\omega_1) L_{zz}(\omega_2) \sin\beta_2 \chi_{yyz} \\ \chi_{eff}^{(2),sps} &= L_{yy}(\omega) L_{zz}(\omega_1) L_{yy}(\omega_2) \sin\beta_1 \chi_{yzy} \\ \chi_{eff}^{(2),pss} &= L_{zz}(\omega) L_{yy}(\omega_1) L_{yy}(\omega_2) \sin\beta \chi_{zyy} \\ \chi_{eff}^{(2),ppp} &= -L_{xx}(\omega) L_{xx}(\omega_1) L_{zz}(\omega_2) \cos\beta \cos\beta_1 \sin\beta_2 \chi_{xxx} \\ &\quad -L_{xx}(\omega) L_{zz}(\omega_1) L_{xx}(\omega_2) \cos\beta \sin\beta_1 \cos\beta_2 \chi_{xzx} \\ &\quad +L_{zz}(\omega) L_{xx}(\omega_1) L_{xx}(\omega_2) \sin\beta \cos\beta_1 \cos\beta_2 \chi_{zxx} \\ &\quad +L_{zz}(\omega) L_{zz}(\omega_1) L_{zz}(\omega_2) \sin\beta \sin\beta_1 \sin\beta_2 \chi_{zzz} \end{aligned} \quad (2)$$

It is so defined that the  $xy$  plane in the laboratory coordinates system  $\lambda(x, y, z)$  is the plane of interface; all

the light beams propagate in the  $xz$  plane;  $p$  denotes the polarization of the optical field in the  $xz$  plane, with  $z$  as the surface normal, while  $s$  the polarization perpendicular to the  $xz$  plane. The consecutive superscript, such as  $ssp$ , represents the following polarization combinations: SFG signal  $s$  polarized, visible beam  $s$  polarized, IR beam  $p$  polarized, and so forth.  $L_{ii}$  ( $i = x, y, z$ ) is the Fresnel coefficient determined by the refractive indexes of the two bulk phase and the interface layer, and the incident and reflected angles.<sup>35,50</sup>  $\chi_{ijk}^{(2)}$  tensors are related to the microscopic hyperpolarizability tensor  $\beta_{i'j'k'}^{(2)}$  of the molecules in the molecular coordinates system  $\lambda'(a, b, c)$  through the ensemble average over all possible molecular orientations.<sup>35,50</sup>

$$\chi_{ijk}^{(2)} = N_s \sum_{i'j'k'} \langle R_{ii'} R_{jj'} R_{kk'} \rangle \beta_{i'j'k'}^{(2)} \quad (3)$$

where  $R_{\lambda\lambda'}(\theta, \phi, \psi)$  is the matrix element of the Euler rotational transformation matrix from the molecular coordination  $\lambda'(a, b, c)$  to the laboratory coordination  $\lambda(x, y, z)$ ;  $\beta_{i'j'k'}^{(2)}$  is the microscopic (molecular) hyperpolarizability tensor.<sup>52,55,60</sup> Here  $N_s$  is the molecular number density at the interface.  $\langle A \rangle$  represents orientational average of property  $A(\theta, \phi, \psi)$  over the orientational distribution function  $f(\theta, \phi, \psi)$ .

$$\langle A \rangle = \frac{\int_0^\pi \int_0^{2\pi} \int_0^{2\pi} A(\theta, \phi, \psi) f(\theta, \phi, \psi) \sin \theta d\theta d\phi d\psi}{\int_0^\pi \int_0^{2\pi} \int_0^{2\pi} f(\theta, \phi, \psi) \sin \theta d\theta d\phi d\psi} \quad (4)$$

For SFG-VS,  $\beta^{(2)}$  is IR frequency ( $\omega_2$ ) dependent,

$$\beta_{i'j'k'}^{(2)} = \beta_{NR, i'j'k'}^{(2)} + \sum_q \frac{\beta_{q, i'j'k'}}{\omega_2 - \omega_q + i\Gamma_q} \quad (5)$$

Thus,  $\chi_{ijk}^{(2)}$  can be expressed into,

$$\chi_{ijk}^{(2)} = \chi_{NR, ijk}^{(2)} + \sum_q \frac{\chi_{q, ijk}}{\omega_2 - \omega_q + i\Gamma_q} \quad (6)$$

Therefore, SFG-VS measures the vibrational spectroscopy of molecular interfaces. For dielectric interfaces, such as liquid interfaces, the non-resonant term  $\beta_{NR, i'j'k'}^{(2)}$  or  $\chi_{NR, ijk}^{(2)}$  is generally negligible compare with the resonant terms.

Recently, we have found that the following formulation is very effective in quantitative polarization and orientation analysis of SFG and SHG data. It can be generally shown that in surface SFG and SHG for an interface with orientational order, the effective second order susceptibility  $\chi_{eff}^{(2)}$  can be simplified into the following form.<sup>49</sup>

$$\chi_{eff}^{(2)} = N_s * d * (\langle \cos \theta \rangle - c * \langle \cos^3 \theta \rangle) = N_s * d * r(\theta) \quad (7)$$

$r(\theta)$  is called the *orientational field functional*, which contains all molecular orientational information at a given SFG experimental configuration; while the dimensionless parameter  $c$  is called the *general orientational parameter*, which determines the orientational response  $r(\theta)$  to the molecular orientation angle  $\theta$ ; and  $d$  is the susceptibility strength factor, which is a constant in a certain experimental polarization configuration with a given molecular system. The  $d$  and  $c$  values are both functions of the related Fresnel coefficients including the refractive index of the interface and the bulk phases, and the experimental geometry.

The key for quantitative analysis is that both  $d$  and  $c$  can be explicitly derived from the expressions of the  $\chi_{eff}^{(2)}$  in relationship to the macroscopic susceptibility and microscopic (molecular) hyperpolarizability tensors for a particular molecular vibrational modes,<sup>50,52</sup> as shown for the water molecules with  $C_{2v}$  symmetry in the appendix. With the parameters  $c$  and  $d$ , the polarization dependence and the orientation dependence of the SFG/SHG signal for a certain interface at certain experimental configuration can be analyzed and calculated with clear physical picture on molecular orientation and orientational distribution.<sup>49</sup> Reciprocally, information on the molecular symmetry, molecular orientation and dynamics can be obtained from the analysis on the SFG intensity relationships measured in different polarization combinations and experimental configurations.<sup>50,51,52,53</sup>

The orientational average in Eq.3 is only the static average on molecular orientations, without considering fast molecular motion effects. Recently Wei *et al.* discussed the fast and slow limit of the time average over orientational motion for  $\chi_{eff}^{(2)}$ , and they also applied this treatment to analysis the polarization dependence of SFG measurement of the OH stretching vibrational spectra for the air/water interface.<sup>25</sup> In the fast motion limit, the orientational motion is faster than the vibrational relaxation time scale  $1/\Gamma_q$  of the  $q$ th vibrational mode; while in the slow motion limit, the orientational motion is much slower than  $1/\Gamma_q$ .

According to Wei *et al.*,<sup>25</sup> the slow motion limit gives,

$$\chi_{ijk}^{(2)} = N_s \sum_q \sum_{i'j'k'} \frac{\beta_{q, i'j'k'}^{(2)}}{\omega_2 - \omega_q + i\Gamma_q} \langle R_{ii'} R_{jj'} R_{kk'} \rangle \quad (8)$$

while the fast motion gives,

$$\chi_{ijk}^{(2)} = N_s \sum_q \sum_{i'j'k'} \frac{\beta_{q, i'j'k'}^{(2)}}{\omega_2 - \omega_q + i\Gamma_q} \langle R_{ii'} R_{jj'} \rangle \langle R_{kk'} \rangle \quad (9)$$

in which  $R_{\lambda\lambda'}(t) = \hat{\lambda} \cdot \hat{\lambda}'(t)$  is the time-dependent direction Euler transformation matrix from  $\lambda'(a, b, c)$  to  $\lambda(x, y, z)$  coordinates system. Because of the molecular orientational motion, the molecular coordinates  $\lambda'(a, b, c)$  is time-dependent. Eq.8 is equivalent to Eq.6, which is obtained by insertion of Eq.5 into Eq.3.

### III. EXPERIMENT

The details of the laser system has been described in our previous reports.<sup>50,56,57</sup> Briefly, the 10Hz and 23 picosecond SFG spectrometer laser system (EKSPLA) is in a co-propagating configuration. The efficiency of the detection system has been improved for the weak SFG signal of air/water interface. A high-gain low-noise photomultiplier (Hamamatsu, PMT-R585) and a two channel Boxcar average system (Stanford Research Systems) are integrated into the EKSPLA system. The voltage of R585 was 1300V in the measurement for air/water interface, and 900V for the Z-cut quartz surface. The wavelength of the visible is fixed at 532nm and the full range of the IR tunability is  $1000cm^{-1}$  to  $4300cm^{-1}$ . The specified spectral resolution of this SFG spectrometer is  $< 6cm^{-1}$  in the whole IR range, and about  $2cm^{-1}$  around  $3000cm^{-1}$ . Each scan was with a  $5cm^{-1}$  increment and was averaged over 300 laser pulses per point. Each spectrum has been repeated for at least several times. Moreover, for *sps* polarization, each spectrum has been repeated for more than a dozen times and averaged. The energy of visible beam is typically less than  $300\mu J$  and that of IR beam less than  $150\mu J$  around  $3000cm^{-1}$  and  $3700cm^{-1}$ , and less than  $100\mu J$  in the region in between. These are comparable to literature reported values for measurement of air/water interface.<sup>20</sup> All measurements were carried out at controlled room temperature ( $22.0 \pm 0.5^\circ C$ ) and humidity (40%). The sample used was ultrapure water from standard Millipore treatment ( $18.2 M\Omega \cdot cm$ ). The whole experimental setup on the optical table was covered in a plastic housing to reduce the air flow. No detectable evaporation effect was observed for SFG spectrum during each scan.

The normalization procedure of the SFG signal in different experimental configurations need to be specifically discussed. The detail of the normalization procedure for a single experimental configuration was presented in Xing Wei's Ph.D. dissertation.<sup>62</sup> However, the difference of coherent length and Fresnel factors with different incident angles in the quartz SFG signal measurements has to be corrected when comparing SFG signal in different experimental configurations. Therefore, the measured spectrum is firstly normalized with the energy of the incident laser beams, and then normalized to the SFG signal of Z-cut quartz (also normalized by the energy of the incident lasers). Then it times with a converting factor between different experimental configurations. This factor contains the influence of the coherent length of Z-cut quartz,<sup>62</sup> the Fresnel coefficients,<sup>62</sup> the  $\chi_{ijk}$  value for Z-cut quartz, and the factor  $\sec^2\beta$  for each experimental configuration. Therefore, the end result is directly proportional to the SFG intensity in Eq.1. If the spectrum in Fig. 1 is divided by the factor  $\sec^2\beta$  and the factor of the PMT efficiency between 1300V and 900V, which is determined as 24.1 in our detection system, and then times the unit factor  $1 \times 10^{-40} V^4 m^{-2}$  which we left out for simplicity of graph presentation, it will give the value for

$|\chi_{eff}^{(2)}|^2$ . For example, the peak at about  $3700cm^{-1}$  in the *ssp* spectra of Config.2 in Fig.1 is about 0.23 unit. After above conversion it gives  $|\chi_{eff}^{(2)}|^2 = 4.7 \times 10^{-40} V^4 m^{-2}$ , matching satisfactorily with the reported value for less than 10% difference.<sup>25</sup>

Even though the normalized intensities are generally consistent with each other, there can be possibly other sources of errors when intensities in different experimental configurations need to be compared. Because the visible and IR beams have different coherent lengths in the Z-cut crystal, and because these coherent lengths vary with different experimental incident angles, one of the most likely error might come from the different focusing parameters with different beam overlapping quality of the visible and IR beams in the Z-cut quartz crystal with different experimental configurations. Therefore, quantitative comparison of the SFG spectral intensities in different polarizations with the same experimental configuration can be more accurate than comparison intensities between different experimental configurations. Even though the latter is a good solution to reduce such relative error associated with different experimental configurations need to be developed.

### IV. RESULTS AND DISCUSSION

#### A. Polarization SFG Spectra of the air/water interface

Firstly we would like to present the polarization SFG spectra of the air/water interface measured in four different experimental configurations.

We have demonstrated recently that the change of the SFG spectra in different polarizations by varying the experimental configurations can be used for quantitative polarization analysis and orientational analysis.<sup>52,53</sup> Here we present in Fig.1 the SFG spectra in the *ssp*, *ppp* and *sps* polarizations on the air/water interface at four experimental configurations with different incident angles for the visible and IR laser beams. They are, Config.1: Visible= $39^\circ$ , IR= $55^\circ$ ; Config.2: Visible= $45^\circ$ , IR= $55^\circ$ ; Config.3: Visible= $48^\circ$ , IR= $57^\circ$ ; Config.4: Visible= $63^\circ$ , IR= $55^\circ$ .

There are four apparent peaks can be identified in the SFG spectra in Fig.1. They are around  $3700cm^{-1}$ ,  $3550cm^{-1}$ ,  $3450cm^{-1}$  and  $3250cm^{-1}$ , respectively. The  $3700cm^{-1}$ ,  $3450cm^{-1}$  and  $3250cm^{-1}$  peaks has been extensively discussed in the SFG literature.<sup>21,22,23,24,37</sup> However, the  $3550cm^{-1}$  peak has been observed, but not yet clearly identified or assigned.<sup>25</sup> The results of global fit of these spectra with four Lorentzian peaks in Eq.6 are listed in Table I. From the fitting results we can see that the peak bandwidths of the  $3550cm^{-1}$ ,  $3450cm^{-1}$  and  $3250cm^{-1}$  peaks are  $77 \pm 11cm^{-1}$ ,  $103 \pm 7cm^{-1}$  and  $89 \pm 9cm^{-1}$ , respectively. Such broad bandwidths indicate that they all belong to different hydrogen bonded O-H stretching vibrational modes. However, the bandwidth

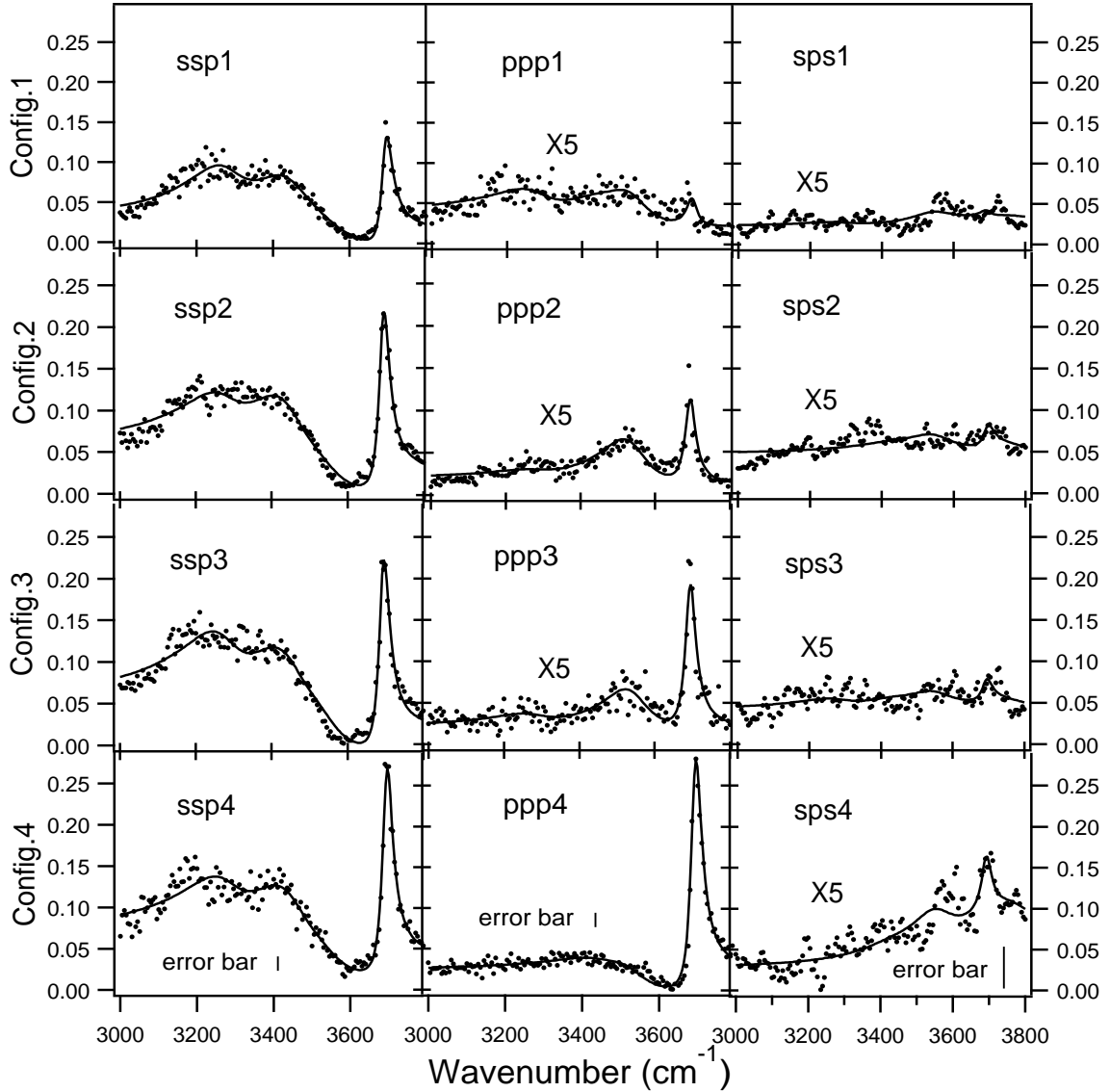


FIG. 1: SFG spectra of air/water interface in different polarization combination and experimental configurations. All spectra are normalized to the same scale. The solid lines are globally fitted curves with Lorentzian line shape function in Eq. 6. Note the different error bars for graphs in different scales.

of the  $3693\text{cm}^{-1}$  peak width is only  $17\text{cm}^{-1}$ , consistent with the symmetric stretching (ss) vibrational mode of the free O-H bond.<sup>20</sup> The signs in Table I contain the information of the relative phase and interference effects of the different vibrational modes. Here the phase of the  $3693\text{cm}^{-1}$  peak is held positive in each fit. Altering the relative phases of the peaks on the same spectrum can not give a reasonable fit. Because we used global fitting with all the spectra, these relative phases can be determined accurately. They can be used to determine the symmetry properties of each vibrational mode in Section IV.C.

According to Eq.2, the *ssp* spectra in different experimental configurations should have the same features from

the  $\chi_{yyz}$  term. As shown in Fig.2, all *ssp* curves overlap quit well when normalized to the  $3693\text{cm}^{-1}$  peak. Calculation of the Fresnel factors with different incident angles can quantitatively explain the relative intensities in all four configurations.<sup>63</sup> Because the SFG spectral intensity from the air/water interface in the OH region is usually several times smaller than that of the C-H region from other air/liquid interfaces, the air/water interface SFG spectra are usually very hard to measure experimentally. Therefore, the well overlapping of the *ssp* spectra in different experimental configurations is a proof for the quality of our SFG-VS data. Furthermore, the spectra we obtained agree very well with these in the literatures.<sup>25,64</sup>

In principle, the *sps* spectra in different experimental

TABLE I: The fitting results of the SFG spectra at air/water interface. The spectra are fitted with Lorentzian line shape function as Eq.6. The peak position of the vibrational modes  $\omega_q$ , the peak width  $\Gamma_q$  and the oscillator strength factor  $\chi_{eff,q,ijk}$  of the vibrational modes are listed. The first column is the fitted value for  $\chi_{NR,eff,ijk}$ . The relative error in fitting of *sps* is larger because of the small signal strength for *sps* spectra.

$\omega_q(cm^{-1})$		3281 $\pm$ 5	3446 $\pm$ 3	3536 $\pm$ 6	3693 $\pm$ 1	
$\Gamma_q(cm^{-1})$		89 $\pm$ 9	103 $\pm$ 7	77 $\pm$ 11	17 $\pm$ 1	
Config.1	ssp	0.17	-6.7 $\pm$ 0.6	-20.1 $\pm$ 1.3	-5.2 $\pm$ 1.2	6.8 $\pm$ 0.2
	ppp	-0.04	3.2 $\pm$ 0.5	2.6 $\pm$ 0.7	5.0 $\pm$ 0.4	1.1 $\pm$ 0.1
	sps	-0.01	-0.1 $\pm$ 0.1	-0.2 $\pm$ 0.1	-3.5 $\pm$ 0.5	0.9 $\pm$ 0.2
Config.2	ssp	0.19	-8.3 $\pm$ 0.6	-24.0 $\pm$ 3.5	-5.0 $\pm$ 3.5	8.5 $\pm$ 0.1
	ppp	-0.02	1.1 $\pm$ 0.5	0.0 $\pm$ 0.8	6.9 $\pm$ 0.3	2.4 $\pm$ 0.6
	sps	0.02	-0.1 $\pm$ 0.1	-0.3 $\pm$ 0.1	-4.5 $\pm$ 0.5	1.6 $\pm$ 0.1
Config.3	ssp	0.22	-10.1 $\pm$ 0.7	-22.8 $\pm$ 1.5	-7.0 $\pm$ 2.0	8.8 $\pm$ 0.2
	ppp	-0.01	2.4 $\pm$ 0.6	0.9 $\pm$ 0.7	6.6 $\pm$ 0.3	2.8 $\pm$ 0.1
	sps	0.01	-0.2 $\pm$ 0.1	-0.3 $\pm$ 0.1	-3.4 $\pm$ 0.7	1.4 $\pm$ 0.2
Config.4	ssp	0.21	-8.8 $\pm$ 0.7	-23.3 $\pm$ 1.4	-5.0 $\pm$ 1.5	9.2 $\pm$ 0.2
	ppp	0.15	-1.0 $\pm$ 0.8	-3.0 $\pm$ 1.3	-9.0 $\pm$ 0.7	9.3 $\pm$ 0.2
	sps	0.01	-0.2 $\pm$ 0.1	-0.4 $\pm$ 0.1	-6.6 $\pm$ 0.8	3.1 $\pm$ 0.2

configurations should also overlap with each other when normalized. However, consistent with the calculations of the corresponding Fresnel factors, the *sps* signal level for Config. 1, 2 and 3 are very close to the noise level, and features in the *sps* spectra can not be clearly identified except for the spectra of Config.4. Therefore, such normalization and comparison for *sps* spectra is not as meaningful as the *ssp* spectra.

Different from the *ssp* and *sps* spectra, the features in the *ppp* spectra in Fig.1 changed drastically with different experimental configurations. This is because that the *ppp* spectra is determined by combination of four different  $\chi_{ijk}$  tensors. Detailed polarization analysis and experimental configuration analysis of these changes in the *ppp* spectra can provide symmetry properties for each spectral features, as well as orientation and structure information of the interfacial molecular groups, as shall be shown later.<sup>50,51,52</sup> We shall show that analysis of the *ppp* spectra in different experimental configurations is very informative. However, this advantage of *ppp* spectra analysis has not been well utilized in the previous literatures.

## B. Orientation and Motion of the Free OH Bond

Now with the knowledge of the SFG vibrational spectra of the air/water interface, we can discuss the orientation and motion of the free O-H bond at the air/water interface.<sup>61</sup>

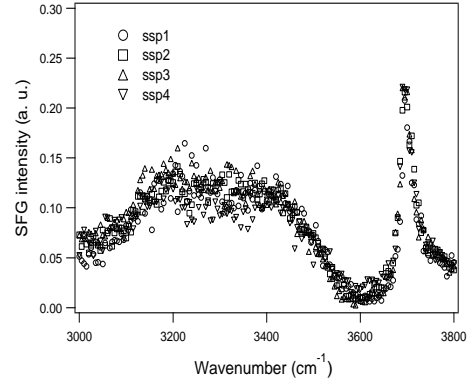


FIG. 2: Overlap of the normalized *ssp* spectra of the air/water interface in different experimental configurations.

The sharp peak around  $3700cm^{-1}$  was generally accepted as the free OH bond protruding out of the liquid water,<sup>20,23,25,66</sup> and it has been treated with  $C_{\infty v}$  symmetry in polarization analysis.<sup>20,25</sup> Wei *et al.* studied the polarization dependence of the intensity of this peak in the *ssp*, *ppp*, and *sps* polarizations measured with experimental configuration of Visible=  $45^\circ$ , IR= $57^\circ$ .<sup>25</sup> Their SFG-VS data are quantitatively very close to our data with Config.2 as expected. Therefore, the *ssp* intensity of the  $3693cm^{-1}$  peak is about 10 times of that of *ppp*, and the *sps* intensity is essentially close zero. Wei *et al.* realized that using the step orientational distribution function in Eq.10, as well as other distribution functions, such as Gaussian, centered at the surface normal, can not explain such *ssp*, *ppp* and *sps* intensity relationships with the slow motion average in Eq.8. On the other hand, the fast motion average centered at the interface normal, as shown in Eq.9 with  $\theta_M = 51^\circ$ , can fairly well explain the observed intensity relationships. Thus, it was concluded that the orientation of the free OH bond of the interfacial water molecule varies over a very broad angular range ( $\theta_M = 51^\circ$ ) within the vibrational relaxation time as short as  $0.5ps$ .<sup>25</sup>

$$\begin{aligned} f(\theta) &= \cos\theta & \text{for } 0 \leq \theta \leq \theta_M \\ f(\theta) &= 0 & \text{for } \theta \geq \theta_M \end{aligned} \quad (10)$$

As shown in Fig.3, Wei *et al.*'s treatment predicts clearly zero intensity for the *sps* spectra at  $3693cm^{-1}$  with the assumption of fast orientational motion centered at the surface normal. Using exactly the same parameters, our calculation of Config.2 gives the same results as that by Wei *et al.* as it should have been.<sup>25</sup> It is clear that the simulation results in Fig.3 can fairly well explain the data in Config. 1, 2 and 3, because all of them have relatively very small *sps* spectral intensity at  $3693cm^{-1}$ . However, even though the fast orientational motion picture can explain the relative intensity between the *ssp* and *ppp* polarization in Config.4, it is clear that it can not explain the apparently non-zero *sps* intensity

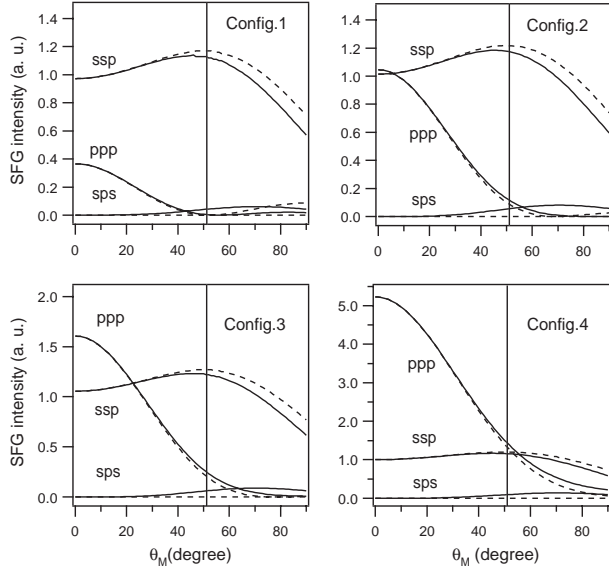


FIG. 3: SFG intensity of the free OH bond simulated with both slow motion limit (solid curves) and fast motion limit (dotted curves) following the procedure and parameters as Wei *et al.*<sup>25</sup>.  $\theta_M$  is the range of orientational motion of the free OH bond. All the curves presented include the factor of  $\sec^2 \beta$ , and all intensities are normalized to the *ssp* intensity in Config.4 with  $\theta_M = 0^\circ$ . The vertical lines indicate the distribution width suggested by Wei *et al.*

at  $3693\text{cm}^{-1}$  with Config.4. As long as the orientation distribution or orientational motion is assumed to be centered to the interface normal,<sup>65</sup> orientational distribution functions other than the step function in Eq.10 give the same conclusion. Since the slow motion limit is already not an option,<sup>25</sup> alternative description of the motion and orientation at the air/water interface has to be invoked.

Because the air/water interface is rotationally isotropic around the interface normal, now we assume that the molecular orientation is centered around the tilt angle  $\theta_0 \neq 0$ , instead of the interface normal ( $\theta_0 = 0$ ). If the Gaussian distribution function is assumed, we have

$$f(\theta) = \frac{1}{\sqrt{2\pi}\sigma^2} e^{-(\theta-\theta_0)^2/2\sigma^2} \quad (11)$$

in which  $\sigma$  is the standard deviation of the angular distribution. We shall show in the followings that by using this distribution function, the  $3693\text{cm}^{-1}$  peak in different polarization and experimental configurations in Fig. 1 can be quantitatively analyzed.

Because the  $3693\text{cm}^{-1}$  peak belongs to the *ss* mode of the free O-H bond at the air/water interface, it has been treated with  $C\infty v$  symmetry. Now we calculate the general orientational parameter  $c$  and the strength factor  $d$  for the *ssp*, *sps* and *ppp* polarizations in all four experimental configurations with the same parameters of the air/water interface as those used by Wei *et al.*<sup>25</sup>

TABLE II: The general orientational parameter  $c$  and the strength factor  $d$  for the vibrational stretching mode of free OH bond in different experimental configurations. The  $d$  value bear the unit  $\beta_{ccc}$  of single OH bond.

	d-ssp	c-ssp	d-sps	c-sps	d-ppp	c-ppp
Config.1	0.274	0.515	0.112	1	-0.154	1.53
Config.2	0.256	0.515	0.118	1	-0.120	2.05
Config.3	0.248	0.515	0.118	1	-0.104	2.43
Config.4	0.176	0.515	0.107	1	-0.035	6.55

The details of the calculation of  $c$  and  $d$  can be found elsewhere.<sup>50,51,52</sup> It is clear from Table II that the  $c$  values for the *ssp* and *sps* polarizations are the same for all four experimental configurations; whereas the  $c$  values of the *ppp* polarization differ significantly for different experimental configurations.

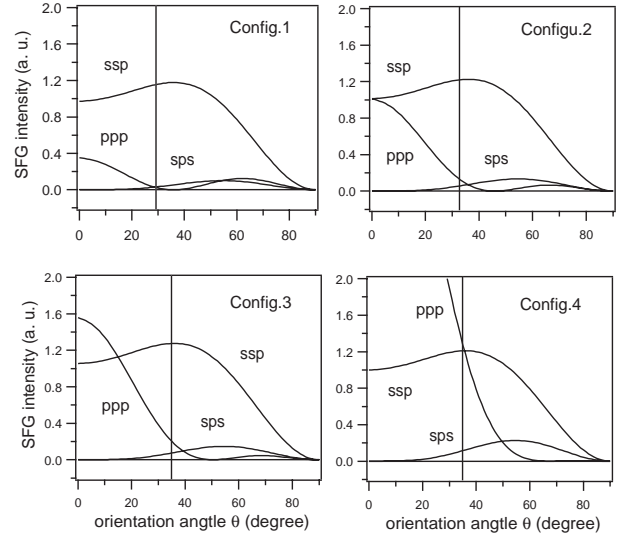


FIG. 4: The simulated SFG intensity of vibrational stretch mode for free OH bond at different orientation angle  $\theta$  assuming  $\sigma = 0^\circ$ . The factor  $\sec^2 \beta$  in Eq.1 is also included for comparison of SFG intensity in different experimental configurations. All curves are normalized to the *ssp* intensity in Config.4 with  $\theta_0 = 0^\circ$ . The vertical lines indicate the orientation which quantitatively explains the observed SFG data.

As we have demonstrated previously,<sup>49,50,51,52</sup> the  $[d * r(\theta)]^2$  vs.  $\theta$  plot with  $\sigma = 0$  in different polarizations can provide direct first look of the physical picture for polarization analysis of SFG-VS data. Here we plot  $[d * r(\theta) * \sec \beta]^2$  vs.  $\theta$  in Fig.4 in order to compare data in different experimental configurations. Thus, the relative intensity for the  $3693\text{cm}^{-1}$  peak in experimental Config.1, 2, 3 and 4 can be used to calculate the orientation angle of the free O-H bond. Using the known procedures<sup>49,50,51,52</sup> and parameters,<sup>25</sup> they give the following four values, i.e.  $28.7 \pm 1.2^\circ$ ,  $32.6 \pm 0.5^\circ$ ,  $34.6 \pm 0.7^\circ$

and  $35.8 \pm 1.0^\circ$ , respectively. These values agree with each other quite well. However, the value from Config.1, whose *ppp* and *sps* intensities are both very weak, is not as reliable as the other three configurations. Averaging over these values gives  $\theta = 33^\circ \pm 1^\circ$ .

It is clear that  $\sigma = 0^\circ$  is not physically possible for the liquid interface. However, the apparent success of the quantitative explanation of the observed SFG spectra of the free O-H bond in different experimental configurations using  $\sigma = 0^\circ$  indicates that the actual  $\sigma$  value can not be very broad. Simulation of the  $3693\text{cm}^{-1}$  peak in different polarizations in each of the four experimental configurations using the Gaussian distribution function in Eq.11 concludes that  $\sigma$  has to be smaller than  $15^\circ$  to satisfy the measured  $3693\text{cm}^{-1}$  peak intensities in all four experimental configurations.  $\sigma = 15^\circ$  is the largest distribution width allowed by the SFG experiment data for a Gaussian orientational distribution function. With  $\sigma = 15^\circ$ , we have  $\theta_0 = 30^\circ$ . This indeed confirms that the orientation of the free O-H bond is within a relatively narrow range (between  $30^\circ$  to  $33^\circ$ ), with a relatively small distribution width ( $\sigma \leq 15^\circ$ ). Calculation with both Eq.8, i.e. slow average limit, and Eq.9, i.e. fast average limit, gives indistinguishable results with  $\sigma$  as small as  $\leq 15^\circ$  if  $\theta_0$  is around  $30^\circ$ . This is because that with a small distribution width, fast and slow motion average should be the same according to Eq.9 and Eq.8. Using a step distribution function around  $\theta_0 \neq 0^\circ$  also give very close orientation angle and distribution width.

Thus, our conclusion of the free O-H orientation and distribution at the air/water interface is drastically different from the conclusion given by Wei *et al.*, which concluded that the free O-H bond orientation varies in a broad range as big as  $102^\circ$  and as fast as 0.5 picosecond, which is the relaxation time for the O-H stretching vibration.<sup>25</sup> It is clear that our conclusion is based on the successful explanation of the observed polarized SFG spectral intensities in different experimental configurations, especially the relatively small but clearly non-vanishing SFG spectral intensity at  $3693\text{cm}^{-1}$  in the *sps* polarization. Our conclusion explicitly supports ultrafast libratory motions with a relatively narrow angular range. As we have known, the dynamics libratory motion of the hydrogen bonding can be as fast as 0.1 picosecond.<sup>67,68</sup> Even with such ultrafast dynamics, the air/water interface is nevertheless well ordered. This is consistent with the generally well ordered picture of the air/liquid and air/liquid mixture interfaces. Recent quantitative analysis of data in SFG vibrational spectroscopy have suggested that vapor/liquid interface are generally well ordered, and sometimes even with anti-parallel double-layered structures<sup>33,56,57,58,63,69</sup>.

It has been generally accepted that liquid interface with strong hydrogen bonding between molecules should be well ordered<sup>33</sup>. Our analysis here not only confirmed this conclusion, but also provided solid and direct experimental measurement of the orientation and motion at the air/water interface.

### C. Polarization Analysis and Determination of Spectral Symmetry Property

Here we try to apply polarization analysis for identifying the symmetry property and for assignment of the SFG vibrational spectra of the air/water interface.

The assignment of the SFG spectra of air/water interface in the range of  $3000$  to  $3800\text{cm}^{-1}$  has been discussed intensively.<sup>21,22,23,24,26,27,28,37,70,71,72</sup> Richmond recently reviewed the current understanding of the bonding and energetics, as well as the SFG spectra assignment, of various aqueous interfaces, including the air/water interface.<sup>27,28</sup> The SFG spectral assignments heavily relied on band fitting of IR and Raman peak positions of bulk water or water cluster spectra,<sup>28</sup> as well as based on theoretical calculations.<sup>8,9,73,74</sup> The sharp peak at about  $3700\text{cm}^{-1}$  has been unanimously assigned to the free O-H stretching vibration mode. The broad peaks around  $3250\text{cm}^{-1}$  and  $3450\text{cm}^{-1}$  undoubtedly belong to the hydrogen bonded O-H stretching modes, but their assignments are not as unanimous as the  $3700\text{cm}^{-1}$  peak. The spectrum around  $3250\text{cm}^{-1}$  was assigned to a continuum of O-H symmetric stretches(ss),  $\nu_1$  of water molecules in a symmetric environment (ss-s), and was generally referred as "ice-like" region because of its similarity in energy to O-H bonds in bulk ice. The broad band around  $3450\text{cm}^{-1}$  was assigned to more weakly correlated hydrogen bonded stretching modes, and was called the "liquid-like" hydrogen-bonded region, where water molecules reside in a more asymmetrically bonded (as) water environment.<sup>27,28</sup> The broad peak around  $3550\text{cm}^{-1}$  appeared clearly in the *ppp* SFG spectra has been identified once and it has not been clearly assigned so far.<sup>25</sup> Shultz *et al.* pointed out that these broad peak should also include the asymmetric stretching mode of water molecules in a symmetry environment and the bending overtone.<sup>24</sup> Richmond *et al.* also suggested that the intensity at about  $3450\text{cm}^{-1}$  include the contribution of donor O-H bond.<sup>26</sup>

Recent progresses on SFG-VS have made it possible to determine the symmetry properties of SFG-VS vibrational spectral features through comparison of SFG spectra in different polarizations and experimental configurations.<sup>50,51,52,53</sup> The key idea of this development is from the commonsense of molecular spectroscopy that vibrational modes of molecular groups with different symmetry properties have different polarization dependence on the interacting optical fields.<sup>75,76</sup> Applying these ideas to polarization analysis of SFG spectra has led to a set of polarization selection rules for different stretching vibrational modes of molecular groups with different molecular symmetry properties, such as stretching vibrational modes of the  $\text{CH}_3$  ( $C_{3v}$ ),  $\text{CH}_2$  ( $C_{2v}$ ) and  $\text{CH}$  ( $C_{\infty v}$ ) groups.<sup>50,51,52</sup> Many of these selection rules are independent from molecular orientation and orientational distribution. Therefore, they can be directly used to identify symmetry property of SFG stretching vibrational band. These progresses make it possible to analyze



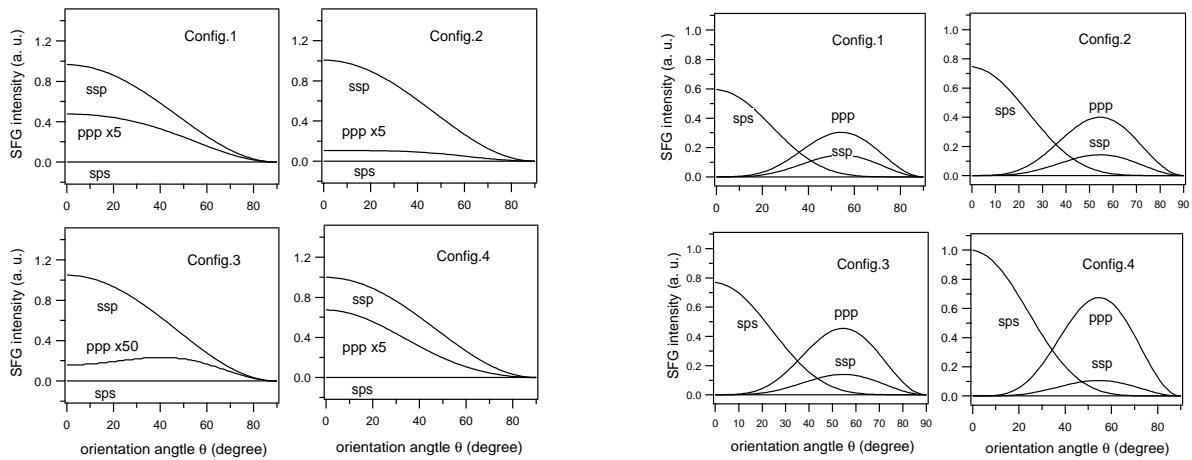


FIG. 5: The simulated SFG intensity for symmetric stretching (*ss*) mode (left) and asymmetric stretching (*as*) mode (right) of water molecule with  $C_{2v}$  symmetry. All curves presented include the factor of  $\sec^2 \beta$ . The intensity of *ss* mode is normalized to the *ssp* intensity in Config.4 with  $\theta = 0^\circ$ . The intensity for *as* mode is normalized to the *sps* intensity in Config.4 with  $\theta_0 = 0^\circ$ . The units between plots of the *ss* and *as* modes differ by 9.11 times according to the  $\beta_{ccc}$  and  $\beta_{aca}$  values in the appendix.

SFG vibrational spectra *in situ*, instead of rely only on the assignments from Raman and IR studies of the bulk phases, which can be called *ex situ*. Because SFG spectra usually has more features than those from IR and Raman measurement, some confusions and errors in the previous spectral assignments have also been clarified.<sup>50,51,52</sup> Even though SFG is naturally a polarized spectroscopy and the interfacial molecular groups are usually ordered, this idea has not been systematically explored until very recently.<sup>49,50,51,52</sup>

Water molecule possesses  $C_{2v}$  symmetry. If the two O-H bond of a water molecule are asymmetrically bonded, both O-H bond has to be treated separately with  $C_{\infty v}$  symmetry. This classification of the water molecule symmetry is generally true no matter it is hydrogen-bonded or not, in cluster, in bulk or at the interface. Therefore, the symmetry property of the SFG vibrational spectra features of the air/water interface can all be classified accordingly. Thus, there are three kind of stretching vibrational modes for us to deal with, namely, the symmetric (*ss*) and asymmetric (*as*) stretching modes for  $C_{2v}$  symmetry, and the stretching mode for  $C_{\infty v}$  symmetry. It is fairly easy to distinguish these three stretching vibrational modes from the polarization selection rules for SFG spectra of  $CH_2$  and  $CH$  groups.<sup>50,51,52</sup> Because the bond angle of the  $CH_2$  group is slightly larger than that of water molecule, the polarization dependence of the  $C_{2v}$  water molecule are slightly different. The key difference is that even when the water molecule at the interface rotate freely around its symmetry axis, the *sps* spectral intensity of its *ss* mode does not vanish as that for  $CH_2$ . However, this fact does not make the polarization selection rules different for the interfacial  $CH_2$  group and the  $C_{2v}$  water molecule.

Two of the major selection rules for the  $C_{2v}$  group at a dielectric interface are: (a) *ssp intensity is always many*

*times of that of ppp for ss mode.* and (b) *ppp intensity for as mode is always several times of that of ssp.* That is to say, if there is any peak which is stronger in the *ssp* than *ppp* spectra, it can not be from the *as* mode.<sup>50,51</sup> These two rules are independent from molecular orientation and orientational distributions at a rotationally isotropic interface.

It is clear from these selection rules, the sharp peak around  $3693cm^{-1}$  in Fig.1 does not belong to the  $C_{2v}$  symmetry, because its intensity in *ppp* polarization in Config. 1,2,3 is smaller than that in *ssp* polarization; while larger in Config.4. On the other hand, these all fits well with the simulations in Fig.4. Therefore,  $3693cm^{-1}$  peak is with  $C_{\infty v}$  symmetry as the free O-H stretching mode. Dissimilarly, both the broad peaks around  $3250cm^{-1}$  and  $3450cm^{-1}$  in Fig.1 are very strong only in the *ssp* spectra in all experimental configurations. They fit well with the *ss* mode of the  $C_{2v}$  symmetry, and can not belong to the *as* mode of the  $C_{2v}$  symmetry, or the  $C_{\infty v}$  symmetry.

It is not so easy to determine the symmetry property of the broad  $3550cm^{-1}$  peak, because it appears to be buried in the high frequency tail of the broad  $3450cm^{-1}$  peak. It is not so straight forward to read its relative intensity in *ssp* and *ppp* polarizations from Fig.1. However, it appears significantly bigger in *sps* polarization in Config.4 than that in Config.1,2,3. Therefore, it appears to fit with the simulations in Fig.4. In order to exclude the possibility that it may belong to a  $C_{2v}$  mode (*ss* or *as*), detailed simulation of the  $C_{2v}$  modes in different polarizations and experimental configurations is now called upon.

As describe in the appendix, the parameter  $c$  and  $d$  of the  $C_{2v}$  vibrational stretching modes are calculated for different polarizations and experimental configurations. Plots of  $[d * r(\theta) * \sec \beta]^2$  vs. tilted angle  $\theta$  of the water

molecule  $c$  axis from the interface normal using these  $c$  and  $d$  values are presented in Fig.5. These plots again confirm that the  $3693\text{cm}^{-1}$  can not belong to any  $C_{2v}$  mode, especially with the one order of magnitude increase of this peak in  $ppp$  polarization.

Clearly, the polarization dependence of the broad  $3550\text{cm}^{-1}$  peak does not fit to the  $ss$  mode of the  $C_{2v}$  symmetry. Otherwise, according to Fig.5, its  $ppp$  intensity in Config.3 has to be about one order of magnitude weaker than that in the observed spectra. This peak can not be the  $as$  mode of the  $C_{2v}$  symmetry either. According to the  $c$  and  $d$  values for the  $as$  mode of the  $C_{2v}$  symmetry, the phases in  $ssp$  and  $ppp$  polarizations have to be with opposite signs in all four experimental configurations. However, fitting of the  $ssp$  and  $ppp$  spectra indicates that in Config.4, the oscillator strengths had the same signs for  $ssp$  and  $ppp$  polarizations, even though in Config. 1,2,3, the oscillator strengths of this peak do possess opposite phases these two polarizations. This indicates that the  $3550\text{cm}^{-1}$  peak is not  $C_{2v}$  symmetry, and it appears to have  $C_{\infty v}$  symmetry.

Because in the bulk phase there is no observation of free O-H bond, and because this broad peak  $3550\text{cm}^{-1}$  appears to be hydrogen-bonded, there is only one possibility that it is the other O-H bond of the interfacial water molecule which has a free O-H bond extruding away from the liquid bulk phase. According to Fig.4, the  $C_{\infty v}$  O-H stretching mode in  $sps$  polarization is about twice as large in Cogfig.4 as that in the other configurations. This is fully consistent with the SFG spectra data in Fig.1 and the fitting results in Table I. Furthermore, in Table I, the phase of the broad  $3550\text{cm}^{-1}$  peak is just opposite to that of the  $3693\text{cm}^{-1}$  peak in both  $ssp$  and  $sps$  polarizations, indicating these two O-H pointing to opposite directions. The phase of the  $ppp$  polarization of the broad  $3550\text{cm}^{-1}$  peak changes signs with different experimental configuration. This is because the orientational angle of the two O-H bonds are some times on the same side of the minimum on the  $ppp$  curves in Fig.4, and sometime on the different side of the minimum, just as predicted with the experimental configuration analysis. These detail features indicated the ability to understand very subtle dependence of the SFG spectra on experimental configurations and the parameters used for the spectra calculations. Further study shall be reported elsewhere.

Further support for the assignment of the broad  $3550\text{cm}^{-1}$  peak came from the IR spectra measurement of the water dimer clusters, where the stretching frequency for the donor O-H bond is just at about  $3550\text{cm}^{-1}$ .<sup>66,70,77,78</sup> This assignment is a good support for our assignment of the peak at  $3550\text{cm}^{-1}$  in  $ppp$  spectra to the single hydrogen-bonded water molecule at the interface. Furthermore, the two O-H stretching vibrations for the methanol dimer are at  $3574\text{cm}^{-1}$  and  $3684\text{cm}^{-1}$ .<sup>79</sup> The donor O-H stretching mode is also in the same region of  $3550\text{cm}^{-1}$ .

There is no observable spectra features in Fig.1 for the

$as$  mode of the  $C_{2v}$  water molecules, neither hydrogen bonded nor non-hydrogen bonded. According to Fig.5, for the  $as$  modes corresponding to the  $ss$  mode around  $3250\text{cm}^{-1}$  and  $3450\text{cm}^{-1}$ , their intensities have to be at least one order of magnitude weaker than that of their corresponding  $ss$  modes. It is understandable that we do not observe them. Above discussion also throw doubts on the existence of interfacial water molecules with two free O-H bonds, as suggested somewhat less convincingly by some recent studies.<sup>13,17,23,26,71</sup> According to the polarization selection rules and the calculation for the polarization dependence of the  $C_{2v}$  water molecules, no detectable spectral features satisfying the  $C_{2v}$  symmetry in the  $3600\text{cm}^{-1}$  and  $3800\text{cm}^{-1}$  has been observed in the SFG spectra.

Here we clearly see that how polarization selection rules, quantitative polarization and experimental configuration analysis can help determine the symmetry property of the observed spectra features. The importance of studying of spectral interference has been demonstrated in recent reports.<sup>23,59,80</sup> Analysis in this work also demonstrated that, in order to discern spectral details, it is useful and effective to analyze the spectral interference of different spectral features through global fitting of SFG spectra in different polarizations and experimental configurations, and to compare fitting results with the prediction from the calculated  $c$  and  $d$  values. This also indicates the usefulness of the formulation of total SFG signal with functions of  $c$  and  $d$  parameters in Eq.7.

#### D. Molecular Structure at Air/Water Interface

With the analysis of the orientation and motion, vibrational spectral symmetry of the water molecules at the air/water interface in above sections, we can have more understanding of the molecular structure of the air/water interface.

In Section IV.B, we have determined that the free O-H oriented around  $30^\circ$  away from the interface normal with a orientational distribution narrower than  $\sigma = 15^\circ$ , and in Section IV.C, we have identified the spectral feature around  $3550\text{cm}^{-1}$  of the other hydrogen bonded O-H bond of this water molecule. If the plane of this interfacial water molecule is close to perpendicular to the interface, the orientation of the hydrogen-bonded O-H should point into the liquid phase with a orientation around  $135^\circ$  away from the interface normal. This orientation is fully consistent with the calculation of the polarization and experimental configuration dependence of the broad  $3550\text{cm}^{-1}$  peak with a  $C_{\infty v}$  symmetry with the observed SFG intensities, detail to be reported elsewhere. Such orientation makes the dipole of this water molecule points around  $97^\circ$  from the interface normal. This picture is fully consistent with conclusions in many previous experimental and theoretical studies,<sup>5,8,13,20,81,82,83,84,85,86,87,88</sup> but certainly different from some.<sup>25</sup>

From Section IV.C, the broad spectral features be-

tween  $3100\text{cm}^{-1}$  to  $3500\text{cm}^{-1}$  are determined to be symmetric stretching modes of the  $C_{2v}$  symmetry. Because the peaks are broad, and their energies is in the range of hydrogen-bonded O-H stretching range, they can only come from the water molecules with two donor O-H bonds, whose oxygen atom can accept either two, one or zero hydrogen atom from other water molecules as hydrogen donors. Certainly, the water molecule with the oxygen atom forming two hydrogen-bonds is tetrahedral in shape and is "ice-like". This is consistent with the previous assignment of the broad  $3250\text{cm}^{-1}$  peak.

The water molecule with no hydrogen bond for the oxygen atom is obviously with  $C_{2v}$  symmetry. However, the water molecule with only one hydrogen bond for the oxygen atom may or may not preserve the  $C_{2v}$  symmetry. However, if this hydrogen bond perturbation to the water structure is limited, this water molecule can still be treated as with  $C_{2v}$  symmetry. The last two kinds of water molecules are certainly not "ice-like", but "liquid-like". The two "liquid-like" species may have slightly different O-H vibrational frequencies. However, only two apparently broad peaks in the  $3100\text{cm}^{-1}$  to  $3500\text{cm}^{-1}$  region have been identified in the literatures.<sup>21,22,23,24,26,27,28,37,70,71,72</sup> More studies on the possible hydrogen-bonded species are certainly warranted in the future.

Here we confirm the conclusion by Brown *et al.* that these  $C_{2v}$  water species all have their dipole vector point out of the bulk liquid phase, i.e. with both hydrogen atoms point into the bulk liquid phase.<sup>23</sup> It is clear in Table I, the signs of the *ssp* polarization oscillator strength factors of the  $C_{2v}$  water species are all in opposite phase to that of the free O-H peak at  $3693\text{cm}^{-1}$  in all experimental configurations. The signs and values of the *c* and *d* parameters of the  $C_{2v}$  and  $C_{\infty v}$  in Table III and Table II, respectively, indicate that the *c* axis of the  $C_{2v}$  species has to be in opposite direction to the *c* axis of the free O-H bond at the interface. Therefore, as defined as in the appendix, the  $C_{2v}$  species have to have their dipole vector point out of the bulk liquid phase. The calculation of the phase of the *ppp* as well as *sps* spectral features are all consistent with this picture.

However, because the SFG spectral intensities of the *ppp* and *sps* polarizations are generally in the noise level in the  $3100\text{cm}^{-1}$  to  $3500\text{cm}^{-1}$  region (Fig.1), it is difficult to determine the range of the orientation angle  $\theta$  of these hydrogen-bonded species relative to the interface normal. The orientational distribution of these  $C_{2v}$  species can be quite broad, different from that for the interfacial water molecules with the free O-H bond. From our simulations, it appears to us that SFG measurement may not be very effective to determine the orientational angle of the  $C_{2v}$  species at the air/water interface, even though it can do very well with the  $C_{\infty v}$  O-H bonds as shown above. However, our recent analysis of the SHG measurement of the neat air/water interface showed that SHG measurement might be able to help determine the orientational angle of the  $C_{2v}$  species, but not the  $C_{\infty v}$

O-H bonds. Recent SHG results indicated that the average orientation of the interfacial  $C_{2v}$  water molecules is about  $40^\circ$  to  $50^\circ$  from the surface normal.<sup>89</sup>

The molecular structure, orientation and dynamics at nonpolar material/water interfaces have been studied by *ab initio* calculation, MD simulation, or them combined.<sup>5,6,7,8,9,10,11,12,13,90,91</sup> It appears that some different conclusions were drawn on the molecular orientation and structure of the air/water interface in different studies.<sup>6,91,92</sup> Nevertheless, many of these studies concluded that the dipole vector of the interfacial water molecules prefers lying parallel to the interface and have one of the O-H bond protrude out of the liquid phase. The majority of the conclusions from theoretical calculations agree satisfactorily with the experimental analysis of ours and previous studies, but all the simulation results were with significantly broader orientational distributions.<sup>5,8,13,81,82,83,84,85,86,87,88</sup> There were reports concluded that some interfacial water molecules have their two O-H bonds projecting into the vapor phase and with oxygen atoms in the liquid phase.<sup>13,93,94,95</sup> However, we have not found explicit spectroscopic evidence for such species at the air/water interface. These all indicate that detailed comparison of the theoretical calculations and the experimental analysis is certainly an important subject in the future studies.

## V. CONCLUSION

Detailed understanding of the air/water interface is important, and can be used for the general understanding of the liquid water structure. In this work, we presented detailed analysis of the SFG vibrational spectra of the air/water interface taken in different polarizations and experimental configurations. Polarization and experimental configuration analysis have provided detailed information on the orientation, structure and dynamics of the water molecules at the air/water interface. The success of these analysis indicated the effectiveness and ability of SFG-VS as a uniquely interface specific spectroscopic probe of liquid interfaces and other molecular interfaces. It also indicates that for the neat air/water interface, as has been studied in the literature for some other simple air/liquid interfaces, the contribution from the interface region dominates the SFG spectra.<sup>47,96,97,98</sup>

Here are major conclusions we have reached for the air/water interface. Firstly, we concluded that the motion of the interfacial water molecules can only be in a limited angular range, instead rapidly varying over a broad angular range in the vibrational relaxation time suggested previously. Secondly, because different vibrational modes of different molecular species at the interface has different symmetry properties, polarization and symmetry analysis of the SFG-VS spectral features can help assignment of the SFG-VS spectra peaks to different interfacial species. These analysis concluded that the narrow  $3693\text{cm}^{-1}$  and broad  $3550\text{cm}^{-1}$  peaks

belong to  $C_{\infty v}$  symmetry, while the broad  $3250\text{cm}^{-1}$  and  $3450\text{cm}^{-1}$  peaks belong to the symmetric stretching modes with  $C_{2v}$  symmetry. Thus, the  $3693\text{cm}^{-1}$  peak is assigned to the free OH, the  $3550\text{cm}^{-1}$  peak is assigned to the single hydrogen bonded OH stretching mode, and the  $3250\text{cm}^{-1}$  and  $3450\text{cm}^{-1}$  peaks are assigned to interfacial water molecules as two hydrogen donors for hydrogen bonding (with  $C_{2v}$  symmetry), respectively. Thirdly, analysis of the SFG-VS spectra concluded that the singly hydrogen bonded water molecules at the air/water interface have their dipole vector direct almost parallel to the interface, and is with a very narrow orientational distribution. The doubly hydrogen bond donor water molecules have their dipole vector point away from the liquid phase. Finally, we did not find any observable evidence for interfacial water molecules with doubly free O-H bonds at the air/water interface.

Many of the conclusions in this work agree well with previous reports, with much more detailed understandings. The conclusion of the narrow range motion of the free O-H bond is different from the literature. The explicit assignment of the broad  $3550\text{cm}^{-1}$  peak and determination of the symmetry property of the hydrogen-bonded O-H stretching modes in the  $3100\text{cm}^{-1}$  to  $3500\text{cm}^{-1}$  region are based on firm evidences. These conclusions as a whole provided a detailed and general picture of the spectroscopy, structure and dynamics of the air/water interface, which can be used for understanding chemical and biological problems related to the ubiquitous water molecule in general. The concepts and approaches used in the analysis in this report can be applied to studying on more complex molecular interfaces.

Recently, extensive efforts with SFG-VS, as well as SHG, experimental studies and theoretical simulations have been devoted to the renewed interests on ion adsorption and the Jones-Ray effect at the air/aqueous solution interfaces.<sup>24,64,74,99,100,101,102,103,104</sup> We suggest that detailed polarization and experimental configuration analysis of the SFG vibrational spectra be applied to these interfaces.

**Acknowledgment.** This work was supported by the Chinese Academy of Sciences (CAS, No.CMS-CX200305), the Natural Science Foundation of China (NSFC, No.20425309) and the Chinese Ministry of Science and Technology (MOST, No.G1999075305). We thank Bao-hua Wu for help derive the bond polarizability derivative model expressions. H.F.W. acknowledges Y. R. Shen for helpful discussions.

#### Appendix: Calculation of $d$ and $c$ Parameters for $C_{2v}$ Molecule

Here we present the expressions to calculate the parameter  $c$  and  $d$  for water molecules with  $C_{2v}$  symmetry using the bond polarizability derivative model first used

by Hirose *et al.*<sup>105,106</sup> The detailed re-derivation of the complete expressions and the effectiveness of the model can be found in a recent review.<sup>52</sup>

The relationship between the Raman depolarization ratio  $\rho$  and the bond polarizability  $r$  for a molecule group with  $C_{2v}$  symmetry was:<sup>52</sup>

$$\rho = \frac{3}{4+20 \frac{(1+2r)^2}{(1-r)^2(1+3\cos^2\tau)}} \quad (12)$$

in which  $\tau$  is the H-O-H bond angle between the two OH bonds of a water molecule. With the Raman depolarization ratio measured as about 0.03,<sup>107</sup> the bond polarizability  $r$  for OH bond in water molecule can be deduced to be 0.32, as used by Du *et al.*<sup>20</sup>

The 7 hyperpolarizability tensor elements of water molecule with  $C_{2v}$  symmetry are as the followings.

$$\begin{aligned} \beta_{aac} &= \frac{G_a \beta_{OH}^0}{\omega_{a1}} [(1+r) - (1-r) \cos \tau] \cos(\frac{\tau}{2}) \\ \beta_{bbc} &= \frac{2G_a \beta_{OH}^0}{\omega_{a1}} r \cos(\frac{\tau}{2}) \\ \beta_{ccc} &= \frac{G_a \beta_{OH}^0}{\omega_{a1}} [(1+r) + (1-r) \cos \tau] \cos(\frac{\tau}{2}) \\ \beta_{aca} &= \beta_{caa} = \frac{G_b \beta_{OH}^0}{\omega_{b1}} [(1-r) \sin \tau] \sin(\frac{\tau}{2}) \\ \beta_{bcb} &= \beta_{cbb} = 0 \end{aligned} \quad (13)$$

Where  $G_a = (1 + \cos \tau)/M_O + 1/M_H$  and  $G_b = (1 - \cos \tau)/M_O + 1/M_H$  are the inverse effective mass for the symmetric ( $a_1$ ) and asymmetric ( $b_1$ ) normal modes, with  $M_O$  and  $M_H$  as the atomic mass of O and H atoms, respectively.  $\omega_{a1}$  and  $\omega_{b1}$  are the vibrational frequencies of the respective modes.  $\beta_{OH}^0 = \frac{1}{2\varepsilon_0} \alpha'_{\zeta\zeta} \mu'_\zeta$ , as defined by Wei *et al.*<sup>48</sup> The water molecule are fixed in the molecular coordination  $\lambda'(a, b, c)$  with the O atom at the coordination center, the molecule plane in  $ac$  plane, and the bisector from the oxygen to the two hydrogen atoms side is the  $c$  axis.

For the achiral rotationally isotropic ( $C_{\infty v}$ ) liquid interface, the symmetric stretching ( $ss$ ,  $a_1$ ) vibrational modes have,<sup>52</sup>

$$\begin{aligned} \chi_{xxz}^{(2),ss} &= \chi_{yyz}^{(2),ss} \\ &= \frac{1}{2} N_s [\langle \cos^2 \psi \rangle \beta_{aac} + \langle \sin^2 \psi \rangle \beta_{bbc} + \beta_{ccc}] \langle \cos \theta \rangle \\ &\quad + \frac{1}{2} N_s [\langle \sin^2 \psi \rangle \beta_{aac} + \langle \cos^2 \psi \rangle \beta_{bbc} - \beta_{ccc}] \langle \cos^3 \theta \rangle \\ \chi_{xxx}^{(2),ss} &= \chi_{zzx}^{(2),ss} = \chi_{zyy}^{(2),ss} = \chi_{zyy}^{(2),ss} \\ &= -\frac{1}{2} N_s [\langle \cos \theta \rangle - \langle \cos^3 \theta \rangle] \\ &\quad [\langle \sin^2 \psi \rangle \beta_{aac} + \langle \cos^2 \psi \rangle \beta_{bbc} - \beta_{ccc}] \\ \chi_{zzz}^{(2),ss} &= N_s [\langle \sin^2 \psi \rangle \beta_{aac} + \langle \cos^2 \psi \rangle \beta_{bbc}] \langle \cos \theta \rangle \\ &\quad - N_s [\langle \sin^2 \psi \rangle \beta_{aac} + \langle \cos^2 \psi \rangle \beta_{bbc} - \beta_{ccc}] \langle \cos^3 \theta \rangle \end{aligned} \quad (14)$$

And the asymmetric stretching ( $as$ ,  $b_1$ ) vibrational modes have,

$$\begin{aligned}
\chi_{xxz}^{(2),as} &= \chi_{yyz}^{(2),as} = -N_s \beta_{aca} \langle \sin^2 \psi \rangle [\langle \cos \theta \rangle - \langle \cos^3 \theta \rangle] \\
\chi_{xzx}^{(2),as} &= \chi_{zxx}^{(2),as} = \chi_{yzy}^{(2),as} = \chi_{zyy}^{(2),as} \\
&= \frac{1}{2} N_s \beta_{aca} [\langle \cos^2 \psi \rangle - \langle \sin^2 \psi \rangle] \langle \cos \theta \rangle \\
&\quad + N_s \beta_{aca} \langle \sin^2 \psi \rangle \langle \cos^3 \theta \rangle \\
\chi_{zzz}^{(2),as} &= 2N_s \beta_{aca} \langle \sin^2 \psi \rangle [\langle \cos \theta \rangle - \langle \cos^3 \theta \rangle] \quad (15)
\end{aligned}$$

The  $b_2$  asymmetric mode are SFG inactive since the hyperpolarizability tensors  $\beta_{bcb}$  and  $\beta_{cbb}$  are zero.

The Euler angel  $\psi$  can be integrated if the H-X-H plane of the  $\text{XH}_2$  group can rotate freely around its symmetry axis  $c$ . For water molecules with both OH bond hydrogen bonded to neighboring molecules in liquid phase, the Euler angel  $\psi$  should not be a fixed value. Assuming a random  $\psi$  distribution we have the following non-vanishing tensor elements for the symmetric-stretching mode.,<sup>50,52</sup>

$$\begin{aligned}
\chi_{xxz}^{(2),ss} &= \chi_{yyz}^{(2),ss} = \frac{1}{4} N_s (\beta_{aac} + \beta_{bbc} + 2\beta_{ccc}) \langle \cos \theta \rangle \\
&\quad + \frac{1}{4} N_s (\beta_{aac} + \beta_{bbc} - 2\beta_{ccc}) \langle \cos^3 \theta \rangle \\
\chi_{xzx}^{(2),ss} &= \chi_{zxx}^{(2),ss} = \chi_{yzy}^{(2),ss} = \chi_{zyy}^{(2),ss} \\
&= -\frac{1}{4} N_s (\beta_{aac} + \beta_{bbc} - 2\beta_{ccc}) (\langle \cos \theta \rangle - \langle \cos^3 \theta \rangle) \\
\chi_{zzz}^{(2),ss} &= \frac{1}{2} N_s (\beta_{aac} + \beta_{bbc}) \langle \cos \theta \rangle \\
&\quad - \frac{1}{2} N_s (\beta_{aac} + \beta_{bbc} - 2\beta_{ccc}) \langle \cos^3 \theta \rangle \quad (16)
\end{aligned}$$

And the non-vanishing tensor elements for water asymmetric-stretching modes are,

$$\begin{aligned}
\chi_{xxz}^{(2),as} &= \chi_{yyz}^{(2),as} = -\frac{1}{2} N_s \beta_{aca} (\langle \cos \theta \rangle - \langle \cos^3 \theta \rangle) \\
\chi_{xzx}^{(2),as} &= \chi_{zxx}^{(2),as} = \chi_{yzy}^{(2),as} = \chi_{zyy}^{(2),as} = \frac{1}{2} N_s \beta_{aca} \langle \cos^3 \theta \rangle \\
\chi_{zzz}^{(2),as} &= N_s \beta_{aca} (\langle \cos \theta \rangle - \langle \cos^3 \theta \rangle) \quad (17)
\end{aligned}$$

For  $\text{CH}_2$  group, there is a general relationship  $\beta_{aac} + \beta_{bbc} - 2\beta_{ccc} \cong 0$ , because  $\tau = 109.5^\circ$ .<sup>50,52</sup> This relationship makes  $\chi_{xxz}^{(2),ss} = \chi_{zxx}^{(2),ss} = \chi_{yzy}^{(2),ss} = \chi_{zyy}^{(2),ss} \cong 0$ , which means that the  $ss$  vibrational mode should vanish in the  $sps$  and  $pss$  polarizations according to Eq. 16. For water molecule,  $\tau = 104.5^\circ$ . Then hyperpolarizability tensors of the water molecule are as the followings:  $\beta_{aac} = 1.296$ ;  $\beta_{bbc} = 0.557$ ;  $\beta_{ccc} = 1$ ;  $\beta_{aca} = \beta_{caa} = 0.741$ ;  $\beta_{bcb} = \beta_{cbb} = 0$ . Here all value are normalized to  $\beta_{ccc} = 1$ . Then,  $\beta_{aac} + \beta_{bbc} - 2\beta_{ccc} = -0.147$ . This value is not 0,

but is very small. So the  $ss$  vibrational mode spectra in the  $sps$  and  $pss$  polarizations should vanish as the  $\text{CH}_2$  group mentioned above. However, they have to be very

TABLE III: The general orientational parameter  $c$  and the strength factor  $d$  for  $ss$  mode and  $as$  mode of water molecule with  $C_{2v}$  symmetry in different polarization combinations. The  $d$  values bear the unit  $\beta_{ccc}$ .

$ss$ mode	d-ssp	c-ssp	d-sps	c-sps	d-ppp	c-ppp
Config.1	0.400	0.038	0.012	1	-0.146	0.174
Config.2	0.374	0.038	0.013	1	-0.079	0.338
Config.3	0.362	0.038	0.013	1	-0.046	0.589
Config.4	0.257	0.038	0.012	1	0.066	-0.378
$as$ mode	d-ssp	c-ssp	d*c-sps	c-sps	d-ppp	c-ppp
Config.1	-0.154	1	-0.122	$\infty$	0.262	0.98
Config.2	-0.144	1	-0.129	$\infty$	0.272	0.99
Config.3	-0.139	1	-0.128	$\infty$	0.277	0.99
Config.4	-0.099	1	-0.117	$\infty$	0.250	1.01

small comparing with in  $ssp$  spectra. This is fully consistent with the small intensities in the  $sps$  SFG spectra for the  $C_{2v}$  water modes in Fig.1.

With above deduction, and following the procedure in previous report,<sup>51</sup> the general orientational parameter  $c$  and strength factor  $d$  for the symmetric stretching ( $ss$ ) mode and asymmetric stretching ( $as$ ) mode of water molecule in different polarizations and experimental configurations can be calculated (see Table III). The parameters used in the calculation are  $n_1(\omega) = n_1(\omega_1) = n_1(\omega_2) = 1$ ;  $n_2(\omega) = n_2(\omega_1) = 1.34$ ;  $n_2(\omega_2) = 1.18$ ;  $n'(\omega) = n'(\omega_1) = 1.15$ ;  $n'(\omega_2) = 1.09$ , respectively. These parameters are the same as the dielectric constants used for calculation of the air/water interface by Wei *et al.*<sup>25</sup> As we have discussed in our reports,<sup>50,51</sup> polarization analysis with the co-propagating experimental geometry is insensitive to the value of the dielectric constants of the IR frequency.<sup>52,53</sup> Therefore, we used the same refractive constants for the IR frequencies across the whole  $3100\text{cm}^{-1}$  to  $3800\text{cm}^{-1}$  region, and this does not appear to affect our analysis. These  $c$  and  $d$  values are used to calculate the polarization and orientation dependence of the SFG intensity, as well as the interference (phase) of different spectral features in different experimental configurations. These calculations can satisfactorily explain the detailed changes of the observed spectral features, as discussed in the main text.

It is to be noticed that in the above discussion we only used single water molecule parameters. When there is association and clustering of water molecules, as long as the  $C_{2v}$  symmetry preserves, and the H-O-H bond angle does not change significantly, above expressions dictated by symmetry properties should still be valid.

- <sup>1</sup> *Water, A Comprehensive Treatise: The Physics and Physical Chemistry of Water*, edited by F. Franks (Plenum, New York, 1972.)
- <sup>2</sup> H. Luecke, H. T. Richter, and J. K. Lanyi, *Science* **280**, 1934-1937 (1998).
- <sup>3</sup> M. Tarek and D. J. Tobias, *Phys. Rev. Letts.* **88**, 138101 (2002).
- <sup>4</sup> D. Gidalevitz, Z. Q. Huang, and S. A. Rice, *Proc. Natl. Acad. Sci. USA* **96**, 2608-2611 (1999).
- <sup>5</sup> R. M. Townsend and S. A. Rice, *J. Chem. Phys.* **94**, 2207-2218 (1991).
- <sup>6</sup> I. Benjamin, *Phys. Rev. Lett.* **73**, 2083-2086 (1994).
- <sup>7</sup> I. Benjamin, *Chem. Rev.* **96**, 1449-1475 (1996).
- <sup>8</sup> A. Morita and J. T. Hynes, *Chem. Phys.* **258**, 371-390 (2000).
- <sup>9</sup> J. T. Hynes, *J. Phys. Chem. B* **106**, 673-685 (2002).
- <sup>10</sup> A. Perry, H. Ahlborn, B. Spacea, and P. B. Moore, *J. Chem. Phys.* **118**, 8411-8419 (2003).
- <sup>11</sup> S. Paul and A. Chandra, *Chem. Phys. Lett.* **373**, 87-93 (2003).
- <sup>12</sup> S. Paul and A. Chandra, *Chem. Phys. Lett.* **386**, 218-224 (2004).
- <sup>13</sup> I-F. W. Kuo and C. J. Mundy, *Science* **303**, 658-660 (2004).
- <sup>14</sup> A. Braslau, M. Deutsch, P. S. Pershan, A. H. Weiss, J. Als-Nielsen, and J. Bohr, *Phys. Rev. Lett.* **54**, 114-117 (1985).
- <sup>15</sup> A. Braslau, P. S. Pershan, G. Swislow, B. M. Ocko, and J. Als-Nielsen, *Phys. Rev. A* **38**, 2457-2470 (1988).
- <sup>16</sup> H. Yui, H. Fujiwara, and T. Sawada, *Chem. Phys. Lett.* **360**, 53-58 (2002).
- <sup>17</sup> K. R. Wilson, M. Cavalleri, B. S. Rude, R. D. Schaller, A. Nilsson, L. G. M. Pettersson, N. Goldman, T. Catalano, J. D. Bozek, and R. J. Saykally, *J. Phys.: Condens. Matter* **14**, L221-226 (2002).
- <sup>18</sup> M. C. Goh, J. M. Hicks, K. Kemnitz, G. R. Pinto, K. Bhattacharyya, K. B. Eienthal, and T. F. Heinz, *J. Phys. Chem.* **92**, 5074-5075 (1988).
- <sup>19</sup> A. J. Fordyce, W. J. Bullock, A. J. Timson, S. Haslam, R. D. Spencer-Smith, A. Alexander, and J. G. Frey, *Mol. Phys.* **99**, 677-687 (2001).
- <sup>20</sup> Q. Du, R. Superfine, E. Freysz, and Y. R. Shen, *Phys. Rev. Lett.* **70**, 2313-2316 (1993).
- <sup>21</sup> Q. Du, E. Freysz, and Y. R. Shen, *Science* **264**, 826-828 (1994).
- <sup>22</sup> Q. Du, E. Freysz, and Y. R. Shen, *Phys. Rev. Lett.* **72**, 238-241 (1994).
- <sup>23</sup> MacG. Brown, E. A. Raymond, H. C. Allen, L. F. Scatena, and G. L. Richmond, *J. Phys. Chem. A* **104**, 10220-10226 (2000).
- <sup>24</sup> M. J. Shultz, C. Schnitzer, and S. Baldelli, *Int. Rev. Phys. Chem.* **19**, 123-153 (2000).
- <sup>25</sup> X. Wei and Y. R. Shen, *Phys. Rev. Lett.* **86**, 4799-4802 (2001).
- <sup>26</sup> L. F. Scatena, M. G. Brown, and G. L. Richmond, *Science* **292**, 908-912 (2001).
- <sup>27</sup> G. L. Richmond, *Annu. Rev. Phys. Chem.* **52**, 357-389 (2001).
- <sup>28</sup> G. L. Richmond, *Chem. Rev.* **102**, 2693-2724 (2002).
- <sup>29</sup> G. L. Richmond, J. M. Robinson, and V. L. Shannon, *Prog. Surf. Sci.* **28**, 1-70 (1988).
- <sup>30</sup> Y. R. Shen, *Annu. Rev. Phys. Chem.* **40**, 327-50 (1989).
- <sup>31</sup> Y. R. Shen, *Nature* **337**, 519-525 (1989).
- <sup>32</sup> R. M. Corn and D. A. Higgins, *Chem. Rev.* **94**, 107-125 (1994).
- <sup>33</sup> P. B. Miranda and Y. R. Shen, *J. Phys. Chem. B* **103**, 3292-3307 (1999).
- <sup>34</sup> K. B. Eienthal, *Chem. Rev.* **96**, 1343-1360 (1996).
- <sup>35</sup> X. Zhuang, P. B. Miranda, D. Kim, and Y. R. Shen, *Phys. Rev. B* **59**, 12632-12640 (1999).
- <sup>36</sup> Z. Chen, D. H. Gracias, and G. A. Somorjai, *Appl. Phys. B-Lasers Opt.* **68**, 549-557 (1999).
- <sup>37</sup> D. E. Gragson and G. L. Richmond, *J. Phys. Chem. B* **102**, 3847-3861 (1998).
- <sup>38</sup> I. Benjamin, *J. Phys. Chem. B* **109**, (2005), jp044157f. In Press.
- <sup>39</sup> S. Woutersen, U. Emmerichs, and H. J. Bakker, *Science* **278**, 658-660 (1997).
- <sup>40</sup> K. B. Eienthal, *Acc. Chem. Res.* **26**, 636-643 (1993).
- <sup>41</sup> B. C. Garrett, *Science* **303**, 1146-1147 (2004).
- <sup>42</sup> L. J. Richter, T. P. Petrali-Mallow, and J. C. Stephenson, *Opt. Lett.* **23**, 1594-1596 (1998).
- <sup>43</sup> E. L. Hommel, G. Ma, and H. C. Allen, *Anal. Sci.* **17**, 1-5 (2001).
- <sup>44</sup> D. K. Hore, J. L. King, F. G. Moore, D. S. Alavi, M. Y. Hamamoto, and G. L. Richmond, *Appl. Spectro.* **58**, 1377-1384 (2004).
- <sup>45</sup> C. M. Johnson, and E. Tyrode, *Phys. Chem. Chem. Phys.* **7**, 2635-2640 (2005).
- <sup>46</sup> (a) Ekspla Co., Vilnius, Lithuania. <http://www.ekspla.com>; (b) Euroscan Co., Belgium. <http://www.euroscan.be/>
- <sup>47</sup> Y. R. Shen, *Appl. Phys. B* **68**, 295-300 (1999).
- <sup>48</sup> X. Wei, S. C. Hong, X. W. Zhuang, T. Goto, and Y. R. Shen, *Phys. Rev. E* **62**, 5160-5172 (2000).
- <sup>49</sup> Y. Rao, Y. S. Tao, and H. F. Wang, *J. Chem. Phys.* **119**, 5226-5236 (2003).
- <sup>50</sup> R. Lu, W. Gan, B. H. Wu, H. Chen, and H. F. Wang, *J. Phys. Chem. B* **108**, 7297-7306 (2004).
- <sup>51</sup> R. Lu, W. Gan, B. H. Wu, Z. Zhang, Y. Guo, and H. F. Wang, *J. Phys. Chem. B* **109**, 14118-14129 (2005).
- <sup>52</sup> H. F. Wang, W. Gan, R. Lu, Y. Rao, and B. H. Wu, *Int. Rev. Phys. Chem.* In press.
- <sup>53</sup> W. Gan, B. H. Wu, H. Chen, Y. Guo, and H. F. Wang, *Chem. Phys. Lett.* **406**, 467-473 (2005).
- <sup>54</sup> (a) R. Lu, W. Gan, and H. F. Wang, *Chin. Sci. Bull.* **48**, 2183-2187 (2003); (b) R. Lu, W. Gan, and H. F. Wang, *Chin. Sci. Bull.* **49**, 899 (2004).
- <sup>55</sup> H. F. Wang, *Chin. J. Chem. Phys.* **17**, 362-368 (2004).
- <sup>56</sup> H. Chen, W. Gan, B. H. Wu, D. Wu, Y. Guo, and H. F. Wang, *J. Phys. Chem. B* **109**, 8053-8063 (2005).
- <sup>57</sup> H. Chen, W. Gan, R. Lu, Y. Guo, and H. F. Wang, *J. Phys. Chem. B* **109**, 8064-8075 (2005).
- <sup>58</sup> H. Chen, W. Gan, B. H. Wu, D. Wu, Z. Zhang, and H. F. Wang, *Chem. Phys. Lett.* **408**, 284-289 (2005).
- <sup>59</sup> V. Ostroverkhov, G. A. Waychunas, and Y. R. Shen, *Phys. Rev. Lett.* **94**, 046102 (2005).
- <sup>60</sup> Goldstein, H. *Classic Mechanics*, Addison-Wesley Publishing Company, Inc., **1980**; p147.
- <sup>61</sup> W. Gan, D. Wu, Z. Zhang, and H. F. Wang, *Phys. Rev. Lett.* (submitted).
- <sup>62</sup> X. Wei, *Ph.D Dissertation* (Department of Physics, Uni-

- versity of California, Berkeley, 2000).
- <sup>63</sup> (a) C. M. Johnson, E. Tyrode, S. Baldelli, M. W. Rutland, and C. Leygraf, *J. Phys. Chem. B* **109**, 321-328, (2005)  
 (b) E. Tyrode, C. M. Johnson, S. Baldelli, C. Leygraf, and M. W. Rutland, *J. Phys. Chem. B* **109**, 329-341 (2005).
  - <sup>64</sup> D. F. Liu, G. Ma, L. M. Levering, and H. C. Allen, *J. Phys. Chem. B* **108**, 2252-2260 (2004).
  - <sup>65</sup> The dangling OH bond at the (0001) face of the hexagonal ice ( $I_h$ ) points straight up along the interface normal [*Phys. Rev. Lett.*, 2001, 86, 1554]. Since air/water interface SFG spectra has ice-like features as in SFG of the ice surface, it was natural to assume that the free OH bond orientation is centered along the interface normal with a broad distribution. Private communication with Professor Y. R. Shen.
  - <sup>66</sup> R. H. Page, J. G. Frey, Y. R. Shen, and Y. T. Lee, *Chem. Phys. Lett.* **106**, 373-376 (1984).
  - <sup>67</sup> A. Luzar and D. Chandler, *Phys. Rev. Lett.* **76**, 928-931 (1996).
  - <sup>68</sup> C. J. Fecko, J. D. Eaves, J. J. Loparo, A. Tokmakoff, and P. L. Geissler, *Science* **301**, 1698-1702 (2003).
  - <sup>69</sup> Y. L. Yeh, C. Zhang, H. Held, A. M. Mebel, X. Wei, S. H. Lin, and Y. R. Shen, *J. Chem. Phys.* **114**, 1837 (2001).
  - <sup>70</sup> J. R. Schewrer, in *Advances In Infrared and Raman Spectroscopy*, edited by R. J. H. Clark and R. E. Hester (Hyden, Philadelphia, 1978), Vol 5, p149.
  - <sup>71</sup> L. F. Scatena, and G. L. Richmond, *Chem. Phys. Lett.* **383**, 491-495 (2004).
  - <sup>72</sup> E. A. Raymond, T. L. Tarbuck, Mac G. Brown, and G. L. Richmond, *J. Phys. Chem. B* **107**, 546-556 (2003).
  - <sup>73</sup> J. P. Devlin, C. Joyce, and V. Buch, *J. Phys. Chem. A* **104**, 1974-1977 (2000).
  - <sup>74</sup> E. C. Brown, M. Mucha, P. Jungwirth, and D. J. Tobias, *J. Phys. Chem. B* **109**, 7934-7940 (2005).
  - <sup>75</sup> J. Michl and E. W. Thulstrup, *Spectroscopy with Polarized Light* (VCH Publishers Inc., United State, 1995).
  - <sup>76</sup> D. C. Harris and M. D. Bertolucci, *Symmetry and Spectroscopy, An Intruduction to Vibrational and Electronic Spectroscopy* (Dover Publications Inc., New York, 1989).
  - <sup>77</sup> M. V. Thiel, E. D. Becker, and G. C. Pimental, *J. Chem. Phys.* **27**, 486-490 (1957).
  - <sup>78</sup> A. J. Tursi and E. R. Nixon, *J. Chem. Phys.* **52**, 1521-1528 (1970).
  - <sup>79</sup> F. Huiskens, A. Kulcke, C. Laush, and J. M. Lisy, *J. Chem. Phys.* **95**, 3924-3929 (1991).
  - <sup>80</sup> S. J. McGall, P. B. Davies, and D. J. Neivandt, *J. Phys. Chem. B* **108**, 16030-16039 (2004).
  - <sup>81</sup> K. Jaqaman, K. Tuncay, and P. J. Ortoleva, *J. Chem. Phys.* **120**, 926-938 (2004).
  - <sup>82</sup> V. V. Zakharov, E. N. Brodskaya, and A. Laaksonen, *Mol. Phys.* **95**, 203-209 (1998).
  - <sup>83</sup> V. V. Zakharov, E. N. Brodskaya, and A. Laaksonen, *J. Chem. Phys.* **107**, 10675-10683 (1997).
  - <sup>84</sup> V. P. Sokhan and D. J. Tildesley, *Mol. Phys.* **92**, 625-640 (1997).
  - <sup>85</sup> R. S. Taylor, L. X. Dang, and B. C. Garrett, *J. Phys. Chem.* **100**, 11720-11725 (1996).
  - <sup>86</sup> K. A. Motakabbir and M. L. Berkowitz, *Chem. Phys. Lett.* **176**, 61-66 (1991).
  - <sup>87</sup> M. A. Wilson, A. Pohorille, and L. R. Pratt, *J. Phys. Chem.* **91**, 4873-4878 (1987).
  - <sup>88</sup> R. M. Townsend, J. Gryko, and S. A. Rice, *J. Chem. Phys.* **82**, 4391-4392 (1985).
  - <sup>89</sup> W. K. Zhang, D. S. Zheng, H. T. Bian, Y. Guo, and H. F. Wang, *J. Chem. Phys.* (submitted).
  - <sup>90</sup> P. Jedlovsky, Á. Vincze, and G. Horvai, *J. Chem. Phys.* **117**, 2271-2280 (2002).
  - <sup>91</sup> P. Jedlovsky, Á. Vincze, and G. Horvai, *Phys. Chem. Chem. Phys.* **6**, 1874-1879 (2004).
  - <sup>92</sup> M. Matsumoto, and Y. Kataoka, *J. Chem. Phys.* **88**, 3233-3245 (1987).
  - <sup>93</sup> B. Yang, D. E. Sullivan and C. G. Gray, *J. Phys.: Condens. Matter* **6**, 4823-4842 (1994).
  - <sup>94</sup> S. B. Zhu, T. G. Fillingim, and G. W. Robinson, *J. Phys. Chem.* **95**, 1002-1006 (1991).
  - <sup>95</sup> C. A. Croton, *Physica* **106A**, 239-259 (1981).
  - <sup>96</sup> X. Wei, S. C. Hong, A. I. Lvovsky, H. Hermann, and Y. R. Shen, *J. Phys. Chem. B* **104**, 3349-3354 (2000).
  - <sup>97</sup> H. Hermann, A. I. Lvovsky, X. Wei, and Y. R. Shen, *Phys. Rev. B* **66**, 205110 (2002).
  - <sup>98</sup> R. Superfine, J. Y. Huang, and Y. R. Shen, *Phys. Rev. Lett.* **66**, 1066-1069 (1991).
  - <sup>99</sup> M. J. Shultz, S. Baldelli, C. Schnitzer, and D. Simonelli, *J. Phys. Chem. B* **106**, 5313-5324 (2002).
  - <sup>100</sup> E. A. Raymond and G. L. Richmond, *J. Phys. Chem. B* **108**, 5051-5059 (2004).
  - <sup>101</sup> P. B. Petersen, J. C. Johnson, K. P. Knutsen, and R. J. Saykally, *Chem. Phys. Lett.* **397**, 46-50 (2004).
  - <sup>102</sup> P. B. Petersen and R. J. Saykally, *Chem. Phys. Lett.* **397**, 51-55 (2004).
  - <sup>103</sup> P. B. Petersen and R. J. Saykally, *J. Phys. Chem. B* **109**, 7976-7980 (2005).
  - <sup>104</sup> M. Mucha, T. Frigato, L. M. Levering, H. C. Allen, D. J. Tobias, L. X. Dang, and P. Jungwirth, *J. Phys. Chem. B* **109**, 7617-7623 (2004).
  - <sup>105</sup> C. Hirose, N. Akamatsu, and K. Domen, *J. Chem. Phys.* **96**, 997-1004 (1992).
  - <sup>106</sup> C. Hirose, H. Yamamoto, H. N. Akamatsu, and K. Domen, *J. Phys. Chem.* **97**, 10064-10069 (1993).
  - <sup>107</sup> W. F. Murphy, *Mol. Phys.* **36**, 727-732 (1978).